Earthquake Geotechnical Engineering for Protection and Development of Environment and Constructions – Silvestri & Moraci (Eds)
© 2019 Associazione Geotecnica Italiana, Rome, Italy, ISBN 978-0-367-14328-2

The effect of deep ground Structures on seismic ground motions on the stiff soil layer in the Kanto region, Japan

T. Kurita
Tokyo Electric Power Services Co., Ltd., Tokyo, Japan

Q. Dong
EduScience Research Institute, Kawasaki, Japan

K. Yoshimi
Center of Computational Mechanics Inc., Tokyo, Japan

ABSTRACT: According to an analysis of seismic observation records in the Kanto region, the site characteristics of strong motions on the stiff soil layer in the region differ from place to place. In this study, numerical simulations were conducted to examine the regional characteristics of seismic ground motions on the stiff soil layer in the Kanto region. The spatial distribution of site characteristics of strong motions on the stiff soil layer in the Kanto region is reproduced by 3D numerical simulations. The analysis of the simulation results revealed the following. The subterranean valleys amplify ground motion caused by cyclically interfering waves. Surface waves generated in the basin interfere with the body waves in the edge of the subterranean basin structure.

1 INTRODUCTION

The Kanto region is centrally located on the main island of Japan. The region includes the Tokyo metropolitan area. It consists of a wide plain with deep soil deposits with surrounding mountains. The averaged thickness of sedimentary fill above the seismic bedrock is almost 3km. Moreover, the bedrock geometry is rugged terrain. There are three labyrinthine plates beneath the region. It seems that the tectonic setting forms this distinct sedimentary basin topography.

According to an analysis of seismic observation records in the region, the site characteristics of strong motions on the stiff soil layer in the Kanto region show regional characteristics (Shingaki *et al.*, 2015). Here, stiff soil is defined as the supporting soil layer with a shear wave velocity more than 300m/s. We have investigated the characteristics of seismic ground motions in the region to understand what accounts for this phenomenon (Kurita *et al.*, 2016). Our tentative explanation attributes this to the amplification effects generated by the deep ground structure. In this study, numerical simulations were conducted to examine the regional characteristics of seismic ground motions on the stiff soil layer of the Kanto region. The area from 80km below sea level to the stiff soil layer (Vs = 500 m/s) under the subsurface ground in the region was modeled using 3D finite elements. The validity of the 3D FEM numerical simulation was investigated by comparing the calculated results to the observation records. Then, the correction of the calculated ground motion with respect to distance attenuation was performed to examine the quantitative spatial characteristic of the simulation results. The ground motion models to predict ground motions on stiff soil were developed using the observation records in the target area. A quantitative investigation was conducted on the mechanism for the production of regional site effects on seismic ground motion on the stiff soil layer in the Kanto region.

2 NUMERICAL SIMULATION MODEL AND CONDITIONS

Numerical simulations were carried out using a 3D finite element method and modeled from the focal region to the stiff soil layer (Vs=500m/s) in depth. Figure 1 shows the areas that were targeted in this analysis. The Kanto Plain surrounded by the Tanzawa Mountains, Kanto Mountains, Ashio Mountains and Tsukuba Mountains is modeled. Properties such as P wave velocity, S wave velocity, density and altitude data were obtained from the deep ground data, divided into 32 layers in the depth direction of J-SHIS (http://www.j-shis.bosai.go.jp/en/) published by the National Research Institute for Earth Science and Disaster Resilience. For the ground data deep beyond the seismic bedrock (Vs=3300m/s), we used the standard structural model of "Three-Dimensional Seismic Velocity Structure Beneath Japanese Islands" developed by Matsubara and Obara (2011). This model is a three-dimensional velocity structure model of the crust and the upper mantle under the Japanese archipelago constructed by seismic tomography. Figure 2 shows the Vs distribution of the analytical model. The southwest end of the analysis region shown in Figure 1 is the coordinate origin of the analytical model.

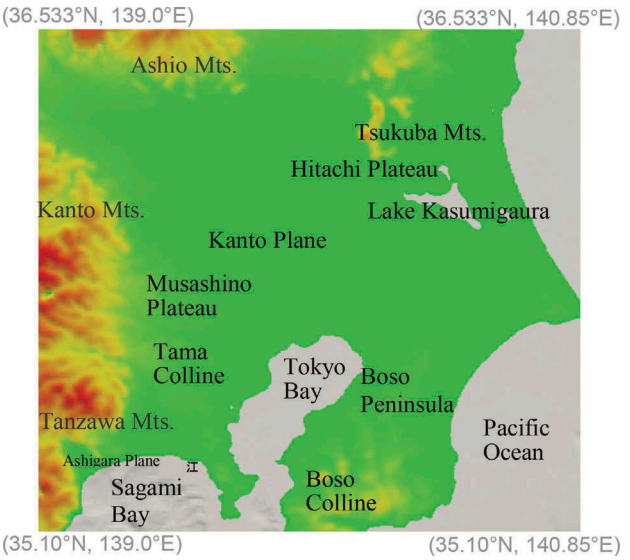

Figure 1. Target area for numerical simulation in the Kanto region.

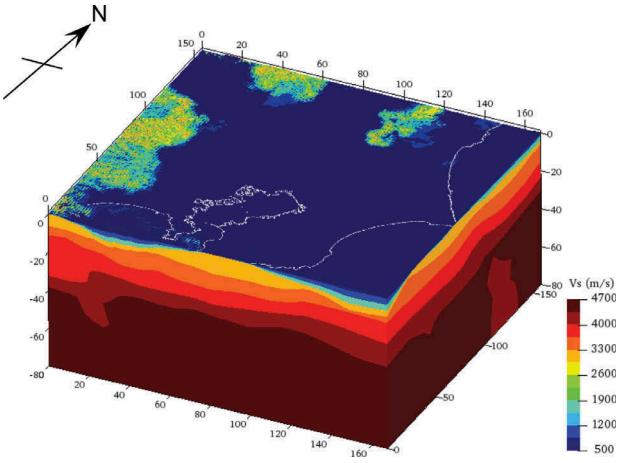

Figure 2. Vs distribution of the numerical simulation model.

Table 1. Configuration of FEM modeling.

Layer No.	Thickness (km)	Division number in depth direction
1	3.5	28
2	6.5	26
3	70.0	140
Specification	Number	
Total node number	74,925,547	
Total element number	Hexahedron:72,508,728/Tetrahedron:7,388,080	

Table 1 shows the configuration of FEM modeling. In this study, we focus attention on long period side ground motions of about 1 second or more, so we decided on the mesh size based on the wave propagation in this period band. The ground was modeled with hexahedron solid elements, and tetrahedral elements were placed at the boundary of the mesh division layers.

Regarding the Q value of the medium, we set the Rayleigh damping so that it is consistent with $Q = 114f^{0.92}$ proposed by Sato and Tatsumi (2002). In addition, we used the model invented by Nakamura and Miyatake (2000) as the source time function.

For the boundary condition, viscous boundaries were allocated by dashpots on both the bottom and the sides. The analysis was numerically integrated in the time domain, and the time step was 0.005 seconds.

3 EVALUATION OF EFFECT OF DEEP GROUND STRUCTURE ON SEISMIC GROUND MOTIONS

3.1 *Ground motion models of target earthquakes*

In this study, in order to investigate distribution characteristics of seismic ground motions in the deep ground structure of the Kanto region, geometric attenuation was corrected for the seismic motions of the simulation results obtained using the 3D finite element method. For that purpose, the attenuation relations of the target earthquakes were modeled using regression analysis. We call this as the ground motion model. The ground motion model is also called the ground motion prediction equation.

Regression analysis of the ground motion models of the acceleration response spectrum (5% damping ratio) was carried out using acceleration records of two horizontal components on the stiff soil layer. In the regression analysis, the data of the observation points of K-NET and KiK-net at 100 points shown in Figure 3 was used. This figure shows the epicenters of three target earthquakes. These earthquakes were selected because they are Mw 5.0 or more occurred within the target area. The inverse response analysis to obtain the ground motions on the stiff soil layer from the observation records on the ground surface were carried out.

The acceleration response spectrum of each observation point used as a target for the regression was taken as the geometric mean value of two horizontal components.

With reference to Joyner and Boor (1981), the following equation, consisting of the distance attenuation term, the internal damping term, and the constant term, describes the ground motion models of the acceleration response spectra.

$$\log Sa(T) = -\log\{r + D(T)\} - B(T) \cdot r + C(T) \pm \sigma(T) \tag{1}$$

Here,

$Sa(T)$: Acceleration response spectrum with 5%damping ratio (cm/s^2)
r : Hypocentral distance (km)

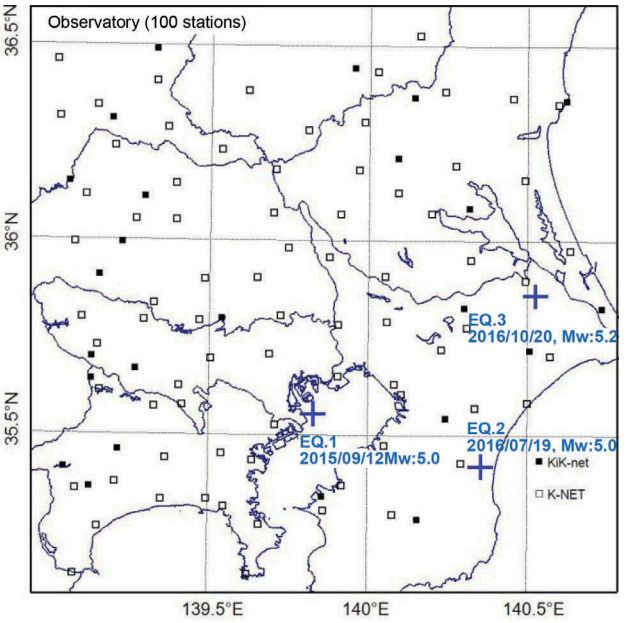

Figure 3. Distribution of observation points and target earthquake epicenters.

T : Period (s)
$B(T)$, $C(T)$, $D(T)$: Regression coefficients
$\sigma(T)$: logarithmic standard deviation on the base 10 logarithms

The value of logarithmic standard deviations on the base 10 logarithms is less than 0.3 in all periodic bands and this can be said to be within the range of sufficient fluctuation.

Figure 4 compares the acceleration response spectra on the stiff soil layer obtained from the observation records and the calculated values by the regression formula. In this figure, the dots are observed values, the solid line represents the average value of the regression equation, and the broken line represents the average value ± the standard deviation of the regression equation. It can be confirmed that the estimated value derived from the regression equation obtained by the regression analysis corresponds well with the observation value.

3.2 *Simulation results*

Using the ground motion models of the target earthquakes obtained from the above investigation, we evaluated the seismic motion distribution at each velocity boundary plane existing in the depth direction of the deep ground structure in the Kanto region as follows.

The horizontal two-component seismic ground motions at each S wave velocity boundary plane of the ground model were extracted. Then, the acceleration response spectrum with 5% damping ratio calculated from the extracted ground motion was divided by the estimated value by the ground motion models. As a result, the geometric attenuation-corrected ground motion characteristic values (response spectrum ratios) were obtained.

The spatial distributions of the response spectral ratios at the velocity boundaries of the deep ground model are shown in Figure 5. The value of the response spectrum ratios shown here are geometric mean values from 1 second to 4 seconds in period. Acceleration time history was output at each velocity boundary surface in increments of 1 km × 1 km in two horizontal directions. The number of output points on each velocity boundary plane is 26,712. In the figure, geometric mean values for all the output points on each velocity boundary surface are also denoted. Here, the seismic moments of the seismic source models were adjusted so

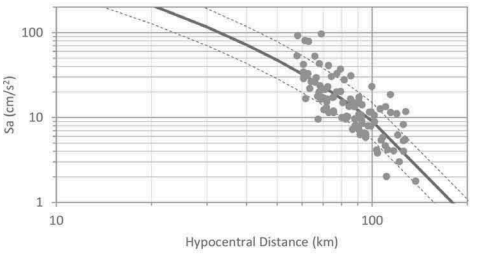

1) EQ.1:2015/09/12, Period:0.02s

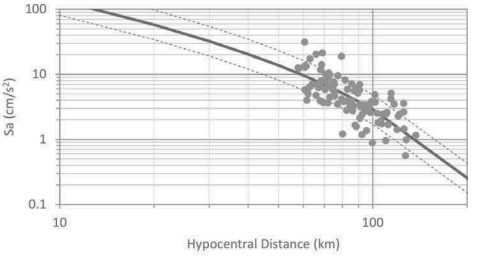

2) EQ.1:2015/09/12, Period:1.0s

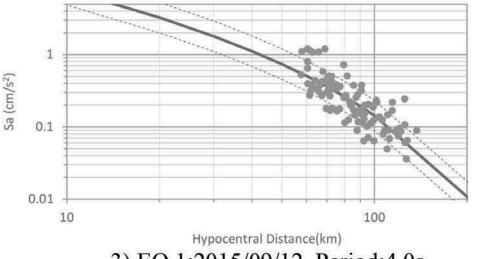

3) EQ.1:2015/09/12, Period:4.0s

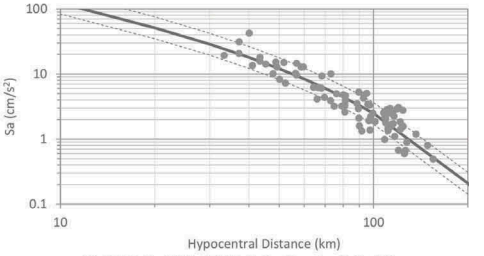

4) EQ.2:2016/07/19, Period:0.02s

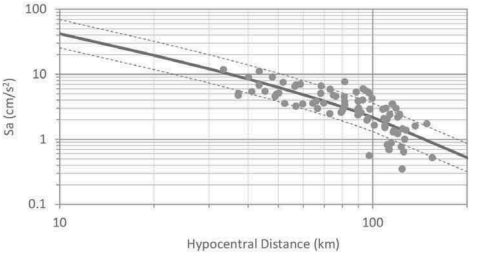

5) EQ.2:2016/07/19, Period:1.0s

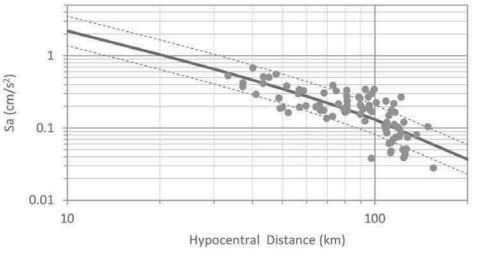

6) EQ.2:2016/07/19, Period:4.0s

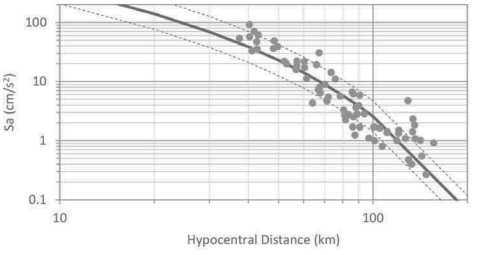

7) EQ.3:2016/10/20, Period:0.02s

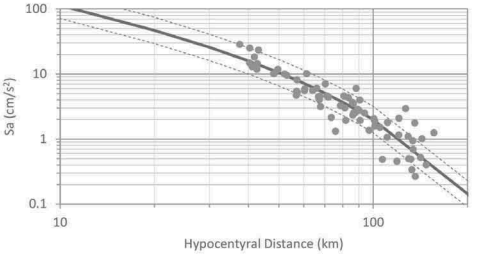

8) EQ.3:2016/10/20, Period:1.0s

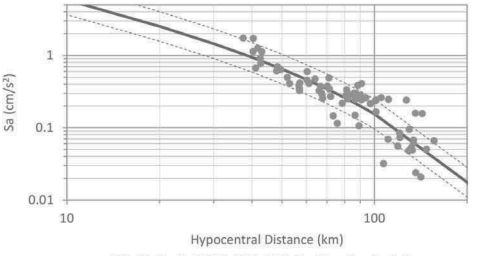

9) EQ.3:2016/10/20, Period:4.0s

Figure 4. Comparison of acceleration response spectra between observed data and estimated values by ground motion model.

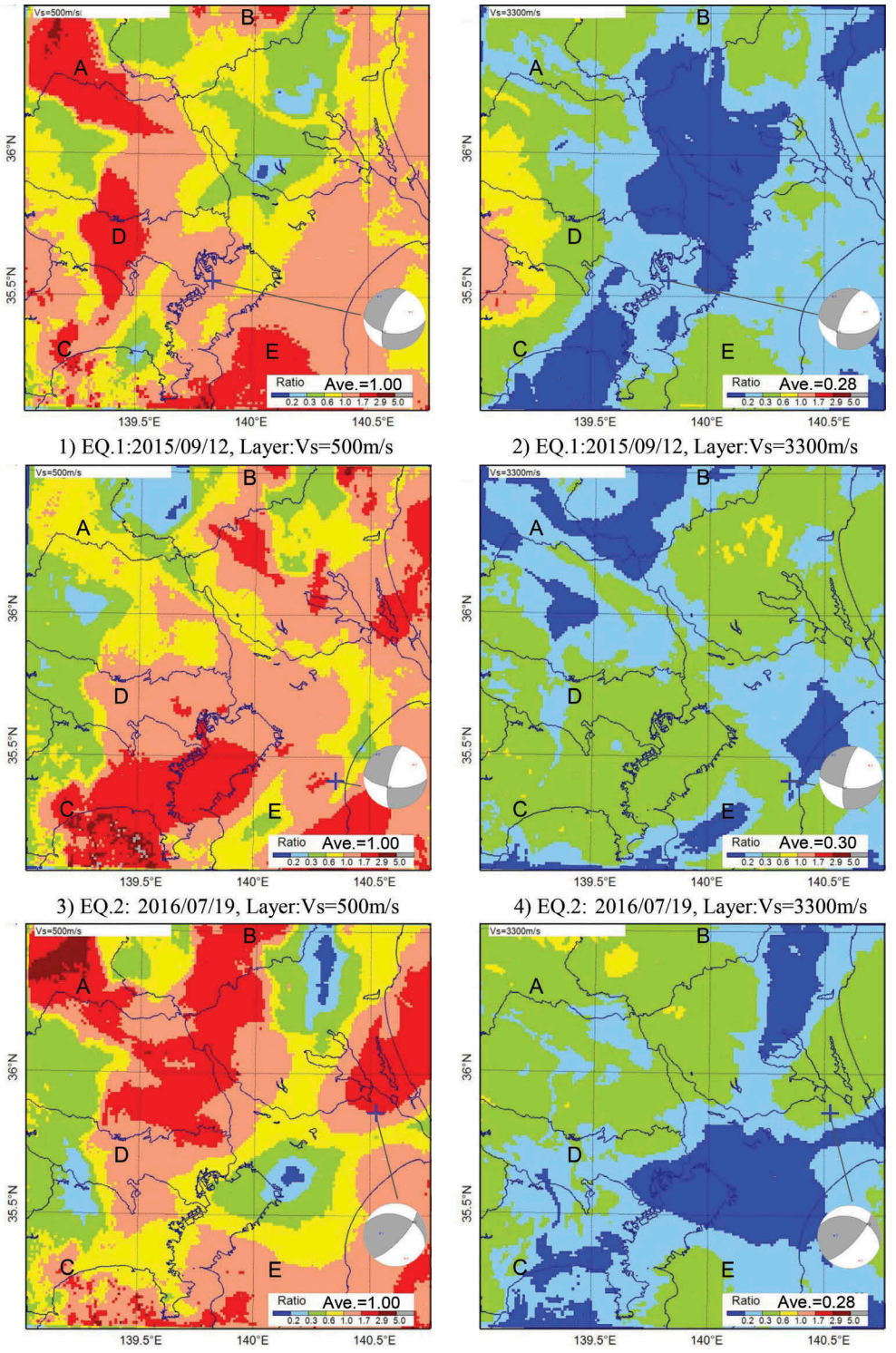

1) EQ.1:2015/09/12, Layer:Vs=500m/s

2) EQ.1:2015/09/12, Layer:Vs=3300m/s

3) EQ.2: 2016/07/19, Layer:Vs=500m/s

4) EQ.2: 2016/07/19, Layer:Vs=3300m/s

5) EQ.3: 2016/10/20, Layer:Vs=500m/s

6) EQ.3: 2016/10/20, Layer:Vs=3300m/s

Figure 5. Distribution of the response spectral ratios at the velocity boundary.

that the time history waveform of the numerical simulation results at the observation points were compatible with the observation records. In this figure, the focal spheres showing the seismic source mechanisms used in numerical simulations are also displayed.

Due to the influence of the ground amplification, the response spectral ratios increase with the top surface of the lower-velocity layer in Figure 5. However, in the Tanzawa Mountains and the Kanto Mountains where the hard rocks are outcrops, there is little difference in the value of the response spectral ratios between the seismic bedrock and the shallow layer. This indicates that the low velocity layer is thin in this area, and the seismic motion in the seismic bedrock reaches the shallow layers almost without amplification. In the case of EQ. 1, the response spectrum ratios in this region are relatively large. This could be one factor because the S wave radiation characteristics are in agreement with the direction in which the maximum amplitude is generated.

3.3 *Discussions*

To figure out the mechanism of the phenomenon by which seismic ground motion causes regionality, local amplification characteristics are taken in detail.

In Figure 5, no clear commonality is seen in the response spectral ratio distribution at the seismic bedrock (Vs=3300 m/s) in any earthquake. On the other hand, it can be seen that the response spectral ratios at the shallower layer (Vs=500 m/s) are large in the five areas common to three target earthquakes. Places showing characteristic trends within the region are indicated by symbols "A" to "E". The areas "A" to "C" in the figure are where the deep ground structures have a valley topography. It is thought that the seismic waves captured in the valley shape are amplified by the repetition of interference at the location of the valley topography in the underground structure.

In the areas of "D" and "E", the underground ground structures are located at the edge of the basin. The seismic ground motions at these areas were amplified by interaction between the body waves and the basin generated surface waves. However, in spite of the existence of similar basin edges other than these two areas, there is no such tendency in other areas. Consequently, the shape of the edge of basin is considered to influence the amplification of surface waves in these areas.

The areas where the amplification becomes large are almost the same in the three earthquakes. However, the amplification factor varies from earthquake to earthquake. This suggests that the amplification factor varies depending on the location and mechanism of the earthquake.

The results of this investigation suggest that the regional characteristics of the long period side seismic ground motion of more than 1 second in the Kanto region is due to the influence of the deep ground structure.

4 CONCLUSIONS

To elucidate the mechanism of the phenomenon in which the seismic ground motion on the stiff soil layer in the Kanto region has regional characteristics, numerical simulations by 3D finite element method were conducted. In this paper, we focused on the effect of deep ground structure on the seismic ground motions of the earthquakes occurred in the south Kanto. The conclusions derived from this study are summarized below.

- To correct the geometric attenuation characteristics of the numerical simulation results, ground motion models of earthquake ground motions at the stiff soil layer were constructed using the observation records of the target three earthquakes.
- Amplification characteristics due to the deep ground structure were able to be evaluated by correcting the geometric attenuation characteristics of the simulation results.
- Amplification of particularly pronounced seismic motion on the stiff soil layer appears in five areas in the Kanto Plain. Three of these are areas sandwiched between mountainous

areas where the underground structure has a valley topography sandwiched between hard ground. The remaining two places are plateaus and hilly areas, where the underground structure is located at the edge of the basin structure.

- It is thought that the seismic waves captured in the valley structure are amplified by the repetition of interference at the location of the valley topography in the underground structure.
- On the edge of the basin structure, it is possible that the seismic ground motions were amplified by interaction between the body waves and the basin-generated surface waves. However, despite the existence of similar basin structure ends other than these two areas, there is no tendency for the seismic ground motion to increase in other areas. Therefore, the shape of the edge of the basin is believed to influence the amplification of the surface waves in these areas.
- Since the hard rocks of the Tanzawa Mountains and the Kanto Mountains are outcrops, it was confirmed that the seismic motion in the seismic bedrock was propagated to the stiff soil layer without amplification.

ACKNOWLEDGEMENTS

In this study, we used observation records from the strong motion observation network (K-NET, KiK-net), deep ground structure data provided by J-SHIS, and earthquake mechanism information from F-net, which were provided by the National Research Institute for Earth Science and Disaster Resilience. Also, we used the JMA unified hypocentral information for seismic source information. The authors express their appreciation to everyone concerned.

REFERENCES

Joyner, W. B. and Boore, D. M. 1981. Peak horizontal acceleration and velocity from strong-motion records including records from the 1979 imperial valley, California, earthquake, *Bulletin of the Seismological Society of America*, Vol. 71, No. 6: 2011–2038.

Kurita, T., Dong Q. and Sato, K. 2016. Ground motion simulation of Kanto region considering 3D ground structure, *Proceedings of the 36th JSCE Earthquake Engineering Symposium*: C11-901. Japan Society of Civil Engineering. (*in Japanese*)

Matsubara, M. and Obara, K. 2011. The 2011 off the Pacific coast of Tohoku Earthquake related to a strong velocity gradient with the Pacific plate, *Earth Planets Space*, Vol.63: 663–667.

Nakamura, H. and Miyatake, T. 2000. An Approximate Expression of Slip Velocity Time Function for Simulation of Near-field Strong Ground Motion, *Zisin*, Vol.53, No.1: 1–11. (*in Japanese*)

Sato, T. and Tatsumi, Y 2002. Source, Path, and Site Effects for Crustal and Subduction Earthquake Inferred from Strong Motion Records in Japan, *Journal of Structural and Construction Engineering*, No.556: 15–24. Architectural Institute of Japan. (*in Japanese*)

Shingaki, Y., Kurita, T., Annaka, T. and Okada, H. 2015. A study on zoning of seismic motion characteristics at engineering base layer of the Kanto plain in Japan, *Journal of Japan Association for Earthquake Engineering*, Vol.15, No.7: 242–252. (*in Japanese*)